Thermochimica Acta, 240 (1994) 235–246
Elsevier Science B.V., Amsterdam
SSDI 0040-6031(94)01681-6

Polymers from renewable resources. Part 3. Thermal analysis of the interpenetrating polymer networks derived from castor oil, polyurethane–polyacrylates

T. Pattnaik [a], P.L. Nayak [a,*], S. Lenka [a], S. Mohanty [b] and K.K. Rao [b]

[a] *Laboratory of Polymers and Fibres, Department of Chemistry, Ravenshaw College, Cuttack-753 003, India*

[b] *Computer Application Group, Regional Research Laboratory, Bhubaneswar-751 013, India*

(Received 14 June 1993; accepted 23 December 1993)

Abstract

A number of polyurethanes (PU) were synthesized by reacting castor oil with hexamethylene di-isocyanate and varying the NCO/OH ratio. All polyurethanes were reacted with acrylamide using EGDM cross-linker and benzoyl peroxide initiator. Thermogravimetric analyses of the polymers were followed, using a computer analysis method, the LOTUS package, for assigning the kinetic mechanism. Various kinetic equations have been used to evaluate the kinetic parameters. The suggested mechanism of degradation of the interpenetrating polymer networks (IPN) are based on the kinetic parameters.

INTRODUCTION

In recent years, the synthesis and characterization of some interpenetrating polymer networks (IPNs) from natural products has attracted the attention of many researchers throughout the world [1–21]. IPNs, in their broadest definition, are materials containing two polymer networks, at least one of whcih is polymerized or cross-linked in the immediate presence of the other. The two polymers can be visualized as being interpenetrating on a molecular level, continuing throughout to the macroscopic level. Hence, both components usually consist of chemically distinct polymers whose immiscibilty and degree of phase separation determine the morphology. The mechanical and morphological properties of these novel polymers have been studied extensively by a larger number of research workers. Theoretical studies to predict their morphological details and physicochemical behaviour have also been reported. A survey of the literature reveals that the thermal properties of this newer type of polymer have not been studied

* Corresponding author.

systematically or intensively. Recently, we have reported [22] the physico-chemical and morphological properties of some IPNs prepared from castor oil, polyurethane–polyacrylates. The present communication presents the thermal behaviour of some of the IPNs that we have prepared. A novel computerized Lotus method has been applied to evaluate various kinetic parameters in order to predict the degradation mechanism [23].

During the past several years, different methods have been used for evaluating kinetic parameters from TG measurements. Sbirrazzuoli et al. [24] have discussed the validity and application of different methods. Zsako [25] developed a method based on standard deviation which mainly deals with comparison of $-\log p(x)$ values at different temperatures and activation energies with $\log g(\alpha)$, and assigns the mechanism for the data with the minimum standard deviation. Although this method is fairly exhaustive it is tedious to use.

Satava and Skvara [26] developed a graphical method for comparison of $\log g(\alpha)$ with $\log p(x)$. This method is based on the principle of the rate of decomposition expressed as

$$\frac{d\alpha}{dt} = kf(\alpha) \tag{1}$$

where $f(\alpha)$ depends on the mechanism and k is the rate constant. The temperature dependence is given by the Arrhenius equation

$$k = Z \exp(-E/RT) \tag{2}$$

where Z is the statistical frequency factor and E the activation energy. Because thermogravimetric analysis is carried out at constant temperature

$$q = \frac{dT}{dt} \tag{3}$$

Combining eqns. (1), (2) and (3)

$$\frac{d\alpha}{f(\alpha)} = \frac{z}{q} \exp\left(-\frac{E}{RT}\right) dt \tag{4}$$

Integration of this equation results in the TG curve [27].

The analytical form of the function $f(\alpha)$ depends on the mechanism of the thermal decomposition. The most general form of this equation is expressed as

$$f(\alpha) = \alpha^a (1-\alpha)^b \tag{5}$$

where a and b are constants called homogeneity factors.

When the analytical function $f(\alpha)$ is known, this leads to a new function $g(\alpha)$. For a known activation energy, Doyle [27] derived the relationship obtained by integration of eqn. (4)

$$g(\alpha) = \frac{ZE}{Rq} p(x) \tag{6}$$

and the function $p(x)$ is given by

$$p(x) = \frac{e^{-x}}{x} - \int_0^{\alpha} \frac{e^{-u}}{u} du \tag{7}$$

where $u = E/RT$ and $x = E/RT_{\infty}$. This function has been tabulated by Zsako [25] for different temperatures and activation energies.

The logarithmic form of eqn. (6) is

$$\log \frac{(ZE)}{(Rq)} = \log g(\alpha) - \log p(x) = \beta \tag{8}$$

where β is independent of temperature.

Whereas Zsako [25] tabulated $-\log p(x)$ values for various temperatures, Satava and Skvara [26] plotted $-\log p(x)$ against T from 0 to 1000°C for comparison. Nair and Madhu Sundrar [28] have shown that the integral kinetic equation makes use of approximations in evaluating the temperature integral and leads to a linear relation between $\log g(\alpha)$ and reciprocal temperature. This procedure has led to a simpler application of regression analysis between $\log g(\alpha)$ and reciprocal temperature, and assigns the kinetic mechanism to the model with a regression value R^2 close to unity.

All these procedures have a number of sequential calculations which have proved to be cumbersome and have resulted in the use of computers in this field. Several packages [29–33] have been developed, mainly using either FORTRAN or BASIC compilers, for the determination of the kinetic mechanism of decomposition. Essentially all these packages are restricted by fixing the pre-exponential factor, activation energy, correlation index, etc. Although graphic representation is widely acceptable for presentation of analysis, these packages lack this ability. Hence, the need for development of a new package is obvious.

Recently, Rao and Mohanty [23] have developed a new LOTUS package for the evaluation of the kinetic parameters of the decomposition of solids.

Spreadsheets with built-in graphics capabilities have been found to be most suitable for this thermogravimetric analysis. To illustrate the capabilities of spreadsheets, LOTUS-123 was chosen for analysis of thermogravimetric data. This package uses the procedure suggested by Nair and Madhu Sundrar [28] which uses regression analysis. The program was written using LOTUS-MACROS for analysis of the nine kinetic models given in Table 1. It has been observed that LOTUS is user friendly and has many built-in capabilities for data processing, such as standard deviation, regression analysis, etc., in addition to its graphic capabilities. As LOTUS runs on menus, this software has an additional advantage over regular compilers, particularly for non-computer professionals. The spreadsheet is built on cells arranged in rows and columns.

Based on this spreadsheet analysis, a package for determining the kinetic mechanism in a non-isothermal process has been developed. Necessary cell

TABLE 1

Kinetic functions (integral differential forms) used for the data analysis

Function	Name of the function	$g(\alpha)$	$f(\alpha)$	Rate-controlling process
D_1	Parabolic law	α^2	$(1/2\alpha)$	One-dimensional diffusion
D_2	Valensi (Barrer) equation	$\alpha + (1-\alpha)\ln(1-\alpha)$	$[-\ln(1-\alpha)]^{-1}$	Two-dimensional diffusion, cylindrical symmetry
D_3	Jander equation	$[1-(1-\alpha)^{1/3}]^2$	$\frac{3}{2}(1-\alpha)^{2/3}[1-(1-\alpha)^{1/3}]^{-1}$	Three-dimensional diffusion, spherical symmetry
D_4	Ginstling–Brounshtein equation	$(1-2/3\alpha)-(1-\alpha)^{2/3}$	$\frac{3}{2}[(1-\alpha)^{-1/3}-1]^{-1}$	Three-dimensional diffusion, spherical symmetry; reaction starting on exterior
F_1	Avrami–Erofeev equation ($n=1$)	$-\ln(1-\alpha)$	$(1-\alpha)$	Assumes random nucleation, one nucleus, one particle
A_2	Avrami–Erofeev equation ($n=2$)	$[-\ln(1-\alpha)]^{1/2}$	$2(1-\alpha)[-\ln(1-\alpha)]^{1/2}$	Assumes random nucleation and its subsequent growth, $n=2$
A_3	Avrami–Erofeev equation ($n=3$)	$[-\ln(1-\alpha)]^{1/3}$	$3(1-\alpha)[-\ln(1-\alpha)]^{2/3}$	Assumes random nucleation and its subsequent growth, $n=3$
R_2	Contracting cylinder	$1-(1-\alpha)^{1/2}$	$2(1-\alpha)^{1/2}$	Phase-boundary reaction, cylindrical symmetry
R_3	Contracting sphere	$1-(1-\alpha)^{1/3}$	$3(1-\alpha)^{2/3}$	Phase-boundary reaction, spherical symmetry

relationships have been used to evaluate different $\log g(\alpha)$ functions for different temperatures. Regression analysis is carried out for $1/T$ and $\log g(\alpha)$. The regression value is given by

$$R^2 = \frac{(XY - n\overline{XY})^2}{(X^2 - n\bar{X}^2)(Y^2 - n\bar{Y}^2)} \tag{9}$$

Slope is given by

$$b = \frac{XY - n\overline{XY}}{X^2 - n\bar{X}^2} \tag{10}$$

and the constant is given by

$$a = \bar{Y} - b\bar{X} \tag{11}$$

where $X = 1/T$ and $Y = \log g(\alpha)$, and n is the number of observations. The mechanism which has R^2 closest to unity is chosen.

The program mainly deals with data entry: the temperature range in °C, the rate of heating q, and the α values. The program evaluates the values for $\log g(\alpha)$ and $1/T$ and carries out regression analysis for $1/T$ versus $\log g(\alpha)$. It saves the results of slopes, constants and R^2 values corresponding to each mechanism, and also plots the graphs for each of the mechanisms and prints out the results.

Based on this LOTUS packaging method, the various kinetic parameters for the degradation of the IPNs listed in Table 2 were calculated and are listed in Tables 3–9.

RESULTS AND DISCUSSION

Figures 1 and 2 indicate that all the IPNs prepared from castor oil, hexamethylene di-isocyanate and acrylamide decompose within 5 wt.% in the temperature range 0–300°C. All the IPNs decompose by about 60% in the range of 300–400°C and by 90–98% in the range 400–500°C. The initial, slow weight loss at around 300°C is attributed to the moisture retained in the samples. The weight loss of about 60% between 300 and 400°C may be attributed to the de-crosslinking of the IPNs. It is pertinent to mention here that the interpenetrating polymer networks contain two or more polymers each in network form. The de-crosslinking occurs between the two network forms in the range 300–400°C. In these types of polymers, one of the polymer networks has been formed or polymerized or cross-linked in the immediate presence of the other. Initially the polyurethanes are formed by the reaction of di-isocyanates with the hydroxyl groups of the ricinoleic acid present in castor oil. This prepolymer (PU) reacts with the vinyl monomer acrylamide in the presence of a free radical initiator, benzoyl peroxide, and a cross-linker, EGDM (ethylene glycol dimethacrylate), to form the IPNs. Hence, the IPNs contain two network polymers, at least one

TABLE 2

Chemical composition and thermal decomposition data of IPNs

Sample	System [a]	Ratio NCO/OH	Composition PU/AM	% wt. loss up to various temps. in °C			O.I. [b]
				100–300	300–400	400–500	
IPN-2	CO + HMDI + AM	1.6	35:65	8	54	95	0.1774
IPN-3	CO + HMDI + AM	1.6	45:55	13	53	94	0.1776
IPN-5	CO + HMDI + AM	1.8	35:65	16	48	96	0.1766
IPN-6	CO + HMDI + AM	1.8	45:55	11	46	90	0.1791
IPN-7	CO + HMDI + AM	2.0	25:75	16	44	89	0.1793
IPN-8	CO + HMDI + AM	2.0	35:65	14	46	91	0.1790
IPN-9	CO + HMDI + AM	2.0	45:55	9	63	96	0.1766

[a] CO = castor oil; HMDI = hexamethylene di-isocyanate; AM = acrylamide. [b] Oxygen index.

TABLE 3

Kinetic parameters calculated by analysis of the α values corresponding to the decomposition of IPN-2 according to the mechanism indicated

$g(\alpha)$	Temp. range in °C	E in kJ mol^{-1}	R^2
D1	300–400	104.78	0.990363
D2	300–400	111.58	0.990439
D3	300–400	119.09	0.990014
D4	300–400	114.08	0.990359
F1	300–400	58.24	0.987319
A2	300–400	23.96	0.981951
A3	300–400	12.53	0.971846
R2	300–400	52.52	0.988433
R3	300–400	54.38	0.988202
D1	410–500	44.03	0.990340
D2	410–500	63.87	0.983144
D3	410–500	98.03	0.958755
D4	410–500	74.65	0.975891
F1	410–500	63.85	0.918617
A2	410–500	25.92	0.883594
A3	410–500	13.28	0.820570
R2	410–500	34.59	0.960988
R3	410–500	43.01	0.948009

TABLE 4

Kinetic parameters calculated by analysis of the α values corresponding to the decomposition of IPN-3 according to the mechanism indicated

$g(\alpha)$	Temp. range in °C	E in kJ mol^{-1}	R^2
D1	300–400	88.03	0.988250
D2	300–400	94.11	0.987746
D3	300–400	100.82	0.986794
D4	300–400	96.34	0.987470
F1	300–400	48.69	0.982682
A2	300–400	19.18	0.973500
A3	300–400	9.35	0.953375
R2	300–400	43.59	0.984463
R3	300–400	45.25	0.983977
D1	410–490	44.59	0.969784
D2	410–490	99.05	0.962861
D3	410–490	99.05	0.940937
D4	410–490	75.48	0.956248
F1	410–490	64.51	0.901712
A2	410–490	26.25	0.860779
A3	410–490	13.50	0.789190
R2	410–490	35.03	0.935758
R3	410–490	43.52	0.925808

TABLE 5

Kinetic parameters calculated by analysis of the α values corresponding to the decomposition of IPN-5 according to the mechanism indicated

$g(\alpha)$	Temp. range in °C	E in kJ mol^{-1}	R^2
D1	300–400	66.05	0.984877
D2	300–400	76.58	0.992560
D3	300–400	91.43	0.990444
D4	300–400	81.37	0.993665
F1	300–400	48.71	0.968188
A2	300–400	18.87	0.951587
A3	300–400	8.92	0.914101
R2	300–400	36.56	0.991505
R3	300–400	40.22	0.988298

TABLE 6

Kinetic parameters calculated by analysis of the α values corresponding to the decomposition of IPN-6 according to the mechanism indicated

$g(\alpha)$	Temp. range in °C	E in kJ mol^{-1}	R^2
D1	300–400	79.33	0.989525
D2	300–400	84.30	0.987025
D3	300–400	89.72	0.983965
D4	300–400	86.10	0.986017
F1	300–400	42.47	0.976618
A2	300–400	16.07	0.962310
A3	300–400	7.27	0.926352
R2	300–400	38.35	0.982080
R3	300–400	39.70	0.980327
D1	410–490	46.76	0.893897
D2	410–490	69.18	0.944236
D3	410–490	110.66	0.984839
D4	410–490	82.07	0.964094
F1	410–490	75.62	0.988353
A2	410–490	31.81	0.983773
A3	410–490	17.20	0.975755
R2	410–490	39.05	0.963793
R3	410–490	49.33	0.980682

of the constituents being polymerized or cross-linked in the immediate presence of the other. From the thermogram, it is evident that there is a sharp decrease in weight loss at around 410°C. This is due to de-crosslinking of the two network forms of the IPNs. A third weight loss occurs in the

TABLE 7

Kinetic parameters calculated by analysis of the α values corresponding to the decomposition of IPN-7 according to the mechanism indicated

$g(\alpha)$	Temp. range in °C	E in kJ mol^{-1}	R^2
D1	300–490	54.16	0.989866
D2	300–490	61.67	0.990768
D3	300–490	70.93	0.988639
D4	300–490	64.72	0.990437
F1	300–490	34.91	0.979838
A2	300–490	11.96	0.963281
A3	300–490	4.31	0.898554
R2	300–490	27.70	0.986648
R3	300–490	29.97	0.985231

TABLE 8

Kinetic parameters calculated by analysis of the α values corresponding to the decomposition of IPN-8 according to the mechanism indicated

$g(\alpha)$	Temp. range in °C	E in kJ mol^{-1}	R^2
D1	300–400	69.13	0.991958
D2	300–400	74.24	0.990960
D3	300–400	79.88	0.989534
D4	300–400	76.12	0.990510
F1	300–400	37.67	0.984863
A2	300–400	13.67	0.973330
A3	300–400	5.67	0.937640
R2	300–400	33.38	0.987451
R3	300–400	34.78	0.986668
D1	410–490	45.88	0.994729
D2	410–490	65.82	0.989801
D3	410–490	57.67	0.967505
D4	410–490	76.55	0.983497
F1	410–490	64.45	0.929674
A2	410–490	26.22	0.899392
A3	410–490	13.48	0.844486
R2	410–490	35.51	0.971971
R3	410–490	43.87	0.959211

range 400–500°C, indicating the complete decomposition of the IPNs at around 500°C. The final weight loss occurs because of the breakage of the bonds in the polymer consisting of the polyacrylamide attached to the ricinoleic acid backbone.

TABLE 9

Kinetic parameters calculated by analysis of the α values corresponding to the decomposition of IPN-9 according to the mechanism indicated

$g(\alpha)$	Temp. range in °C	E in kJ mol^{-1}	R^2
D1	300–400	125.89	0.989424
D2	300–400	134.49	0.991119
D3	300–400	144.17	0.992048
D4	300–400	137.70	0.991557
F1	300–400	71.93	0.990945
A2	300–400	30.80	0.988013
A3	300–400	17.09	0.983207
R2	300–400	64.53	0.990403
R3	300–400	66.92	0.990846
D1	410–490	27.91	0.997970
D2	410–490	45.44	0.993568
D3	410–490	79.18	0.958114
D4	410–490	55.86	0.983756
F1	410–490	55.32	0.898934
A2	410–490	21.66	0.847437
A3	410–490	10.43	0.747305
R2	410–490	25.21	0.984417
R3	410–490	33.59	0.943871

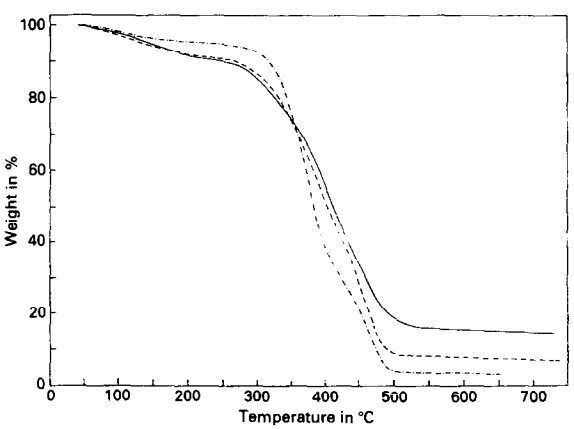

Fig. 1. Weight loss curves of the IPNs: ——, CO + HMDI + AM (NCO:OH, 1.6), (PU:AM, 35:65); – – –, CO + HMDI + AM (NCO:OH, 1.6), (PU:AM, 45:55); – · – ·, CO + HMDI + AM (NCO:OH, 1.8), (PU:AM, 35:65); – · · – · · –, CO + HMDI + AM (NCO:OH, 1.8), (PU:AM, 45:55).

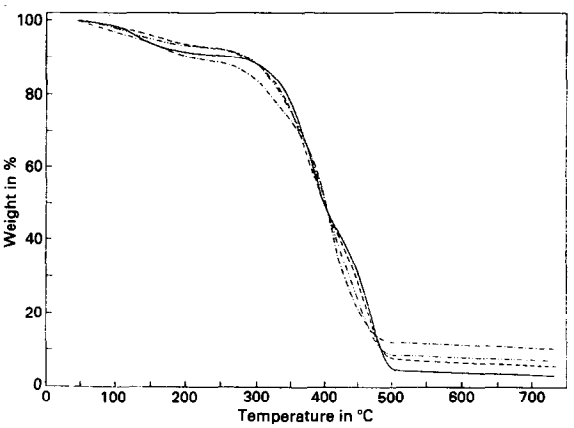

Fig. 2. Weight loss curves of the IPNs: ——, CO + HMDI + AM (NCO:OH, 2.0), (PU:AM, 25:75); – – –, CO + HMDI + AM (NCO:OH, 2.0), (PU:AM, 35:65); – · – · –, CO + HMDI + AM (NCO:OH, 2.0), (PU:AM, 45:55).

Because there are two breaks in the TG curves at around 300–400°C and 410–500°C, the activation energies have been calculated using different mechanisms, taking into account the highest correlation coefficient value, see Tables 3–9.

Specific analytic procedures were not followed, but from the mass of carbonaceous char residue, it can be concluded that the IPNs are not good flame retardants, as evidenced by their oxygen index. Table 2 shows that the oxygen index values are almost the same in all IPNs.

The results indicate that for all the polymers, the activation energy values are considerably higher in the temperature range 300–400°C, than in range 410–500°C. This clearly indicates that the degradation process is slower at 300–400°C and faster at 410–500°C. This is obvious from the structure of the IPNs. The de-crosslinking between the two types of polymers occurs in the temperature range 300–400°C, as mentioned earlier, and because the structure of the IPNs is very complicated, this process is bound to be slower. But in the temperature range 410–500°C, the polyacrylamide attached to the backbone of ricinoleic acid decomposes at a faster rate, and hence the energy of activation is low. These values corroborate the structural decomposition of the IPNs, as predicted by the mechanism. As the IPNs are very complicated in structure, it is very difficult to predict the exact decomposition pathway with temperature increase. Further work to predict the actual method of decomposition is underway.

ACKNOWLEDGEMENT

We greatly acknowledge help rendered from RRL, Bhubaneswar for computer analysis of the TG graphs.

REFERENCES

1 L.H. Sperling, Interpenetrating Polymer Networks and Related Materials, Plenum Press, New York, 1981.
2 L.H. Sperling, Macromol. Rev., 12 (1977) 141.
3 K.C. Frisch, D. Klempner, H.L. Frisch and H. Ghiradella, in L.H. Sperling (Ed.), Recent Advances in Polymer Blends, Grafts, and Blocks, Plenum Press, New York, 1974.
4 G. Allen, M.J. Bowden, G. Lewis, D.J. Blundell and G.M. Jeffs, Polymer, 15 (1974) 13.
5 L.H. Sperling and D.W. Friedman, J. Polym. Sci. Part A2, 7 (1969) 425.
6 H.L. Frisch, D. Klempner and K.C. Frisch, J. Polym. Sci. Part B, 7 (1969) 775.
7 Y.S. Liptov and L.M. Sergeeve, Russ. Chem. Rev. (Engl. Transl.), 45(1) (1976) 63.
8 G.C. Meyer and P.Y. Mehrenberger, Eur. Polym. J., 13 (1977) 383.
9 V. Huelck, D.A. Thomas and L.H. Sperling, Macromolecules, 5 (1972) 340.
10 D. Siegfried and L.H. Sperling, J. Polym. Sci. Polym. Phys. Ed., 16 (1978) 583.
11 L.H. Sperling and R.R. Arnts, J. Appl. Polym. Sci., 15 (1971) 2317.
12 K.C. Frisch, H.L. Frisch, D. Klempner and T. Antczak, J. Appl. Polym. Sci., 18 (1974) 683.
13 R.E. Touhsaent, D.A. Thomas and L.H. Sperling, J. Polym. Sci. Part C, 46 (1974) 175.
14 S.C. Kim, D. Klempner, K.C. Frisch, H.L. Frisch and H. Ghiradella, Polym. Eng. Sci., 15(5) (1975) 339.
15 K.C. Frisch, D. Klempner and S. Migdal, J. Polym. Sci., 12 (1974) 885.
16 N. Devia, J.A. Manson, L.H. Sperling and A. Conde, Polym. Eng. Sci., 18(3) (1978) 200.
17 K.C. Frisch, D. Klempner and S.K. Mukherjee, J. Appl. Polym. Sci., 18 (1974) 689.
18 S.C. Kim, D. Klempner, K.C. Frisch, W. Radigan and H.L. Frisch, Macromolecules, 9 (1976) 258.
19 Valker Huelck, D.A. Thomas and L.H. Sperling, Macromolecules, 5 (1972) 340, 348.
20 A.A. Donatelli, L.H. Sperling and D.A. Thomas, Macromolecules, 9 (1976) 671, 676.
21 D. Klempner, H.L. Frisch and K.C. Frisch, J. Polym. Sci. Part A2, 8 (1970) 921.
22 P.L. Nayak, S. Lenka, S.K. Panda and T. Pattnaik, J. Appl. Poly. Sci., 47 (1993) 1089.
23 K.K. Rao and S. Mohanty, Proc. 8th National Workshop on Thermal Analysis, India, 1991, p. 236.
24 N. Sbirrazzuoli, D. Brunel and L. Elegant, J. Therm. Anal., 38 (1992) 1509.
25 J. Zsako, Kinetic analysis of thermogravimetric data, J. Phys. Chem., 72(7) (1988) 2406–2411.
26 V. Satava and F. Skvara, Mechanisms and kinetics of the decomposition of solids by thermogravimetric method, J. Am. Ceram. Soc., 52 (1969) 591–595.
27 J. Šesták, Review of methods of mathematical evaluation of kinetic data from non-isothermal and isothermal thermogravimetric measurements, Silikaty, 11(2) (1967) 153–190.
28 C.G.R. Nair and C.M. Madhu Sundrar, Thermal decomposition studies: VIII. Dynamic thermogravimetric studies of the mechanism of deamination of some transition metal complexes, Thermochim. Acta, 14 (1976) 373.
29 R.K. Sahoo et al., Computer evaluation of non-isothermal kinetic parameters from TG curves, Thermochim. Acta, 130 (1988) 369–374.
30 Carpes and E. Segal, Basic program to discriminate among mechanisms of solid–gas decompositions (DISCRIM-2), Thermochim. Acta, 185 (1991) 111–127.
31 S. Ma et al., KNIS — A computer program for the systematic kinetic analysis of non-isothermal thermogravimetric data, Thermochim. Acta, 184 (1991) 233–241.
32 M.P. Karran et al., Numerical data for the evaluation of kinetic parameters of solid state decomposition by the non-isothermal method, Thermochim. Acta, 186 (1991) 265–272.
33 S. Mahapatra et al., Thermal decomposition of the hydrolysis products of $Fe(OH)SO_4$, Thermochim. Acta, 161 (1990) 279–285.